Hindawi
Geofluids
Volume 2022, Article ID 2090809, 10 pages
https://doi.org/10.1155/2022/2090809

Research Article

A Coal Bump Risk Assessment and Prediction Model Based on Multiparameter Indices

Tao Luo,[1] **Gangwei Fan**,[1,2] **Shizhong Zhang**,[1] **Shang Ren**,[1] **Yibo Fan**,[1] **and Ruiliang Shen**[1]

[1]*School of Mines, China University of Mining and Technology, No. 1 University Road, Xuzhou, Jiangsu 221116, China*
[2]*State Key Laboratory of Coal Resource and Safe Mining, China University of Mining and Technology, No. 1 University Road, Xuzhou, Jiangsu 221116, China*

Correspondence should be addressed to Gangwei Fan; fangw@cumt.edu.cn

Received 10 October 2021; Accepted 24 February 2022; Published 16 March 2022

Academic Editor: Zhijie Wen

Copyright © 2022 Tao Luo et al. This is an open access article distributed under the Creative Commons Attribution License, which permits unrestricted use, distribution, and reproduction in any medium, provided the original work is properly cited.

Coal bump, a common dynamic disaster in mining of deep coal resources, its assessing and predicting is an important component in safety management. This paper presents a model to assess and predict coal bump risk based on multiparameter indices. A new energy accumulation index S was proposed by considering acoustic emission and electromagnetic emission signal characteristics in mine shocks. Combined with indices E (energy of microseisms) and N (frequency of microseisms) of microseismic monitoring, a static and dynamic coal bump risk assessment and prediction model was established. We studied coal bump events that occurred during extraction in 311305 working face of Bayangale coal mine in Inner Mongolia, China. We obtained the acoustic emission and electromagnetic emission signal distribution and change law, using principal component analysis method and density ellipse to establish the index S. A typical precursory of coal bumps is that AE and EME strength has obvious fluctuation period of 3-4 days, index S showing an obvious decreasing trend, while the time-series curve of the microseismic energy is relatively stable, and the vibration frequency curve has a significant upward trend. After predict the potential coal bump risk and its area of occurrence, large diameter drilling (Φ150 mm) on-site was used to relief pressure concertation in coal seam and roof. The results demonstrate that this model based on multiparameter indices is capable of quantitatively prewarning rock burst risk.

1. Introduction

Coal bumps refers to the dynamic disaster of the instantaneous release of elastic energy accumulated in the coal and rock mass due to the severe instability of coal rock. As an extremely destructive hazard, coal bump can cause roadway deformation, support damage, and even casualties [1–3]. With the increasing demand for coal in China's economic development, the scale and strength of coal mining have improved significantly, and the mining depth has gradually increased. The research shows that the mining depth of coal mines in China extends to the deep at a speed of nearly 20 m per year [4–6]. With the increase of coal mining strength and average mining depth, the coal rock dynamic behavior induced by deep mining (such as coal bumps) is more frequent [7–9]. In the past ten years, more than 660 coal bump accidents occurred in coal mines with coal bump risk of China, and 224 deaths were caused in total [10, 11]. Figure 1 shows the relationship between China's coal production and the number of coal bump mines. As of February 2021, 138 mines with coal bump risk are still in production in China, which poses a great threat to coal mines production and the safety of miners.

The mechanism of coal bump has been expounded from the widely accepted theories, such as "strength theory", "energy theory", "stiffness theory," and "coal bump proneness theory" [13–19]. According to the strength theory, the failure of coal rock is not only affected by stress concentration but also closely related to the ratio of coal strength to rock strength. In the stiffness theory, it is believed that the necessary condition for coal bump is that the stiffness of rock mass structure is greater than that of the loading

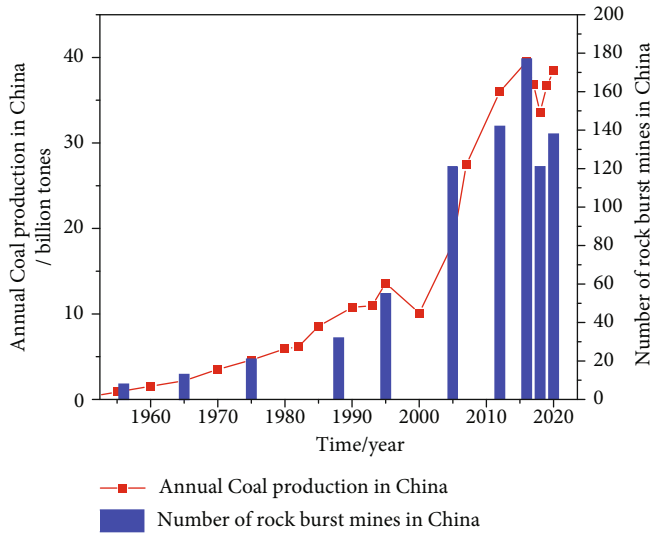

Figure 1: Annual coal production and the number of coal bump mines in China [12].

system. According to the energy theory, when the energy released by the mechanical equilibrium failure of the surrounding rock system is greater than the energy consumed in the system, the coal bump can be caused. In the coal bump proneness theory, it is claimed that the main condition of coal bump is that the tendency of coal rock is greater than its limit value. Based on the engineering practice, "coal bump strength weakening impact theory," "stress control theory," and "disturbance response instability theory" have also been proposed [20–22]. Besides, researchers have studied the impact failure of coal rock combination by laboratory test and numerical simulation and analyzed the dynamic failure process and failure mechanism of surrounding rock in the roadway under impact load [23–25]. Fan et al.'s [26] mechanism of roof shock in longwall coal mining under surface gully: the above researches reveal the initiation mechanism and disaster-causing process of coal bump from different angles. How successful application of the above results to the field of early warning on coal bumps has become the focus of current research.

At present, the main monitoring methods used in the early warning of coal bumps can be divided into drilling yield tests, acoustic emission and electromagnetic emission, microseismic monitoring, and seismic velocity tomography method [27–33]. Coal bump monitoring and early warning technology has a positive guiding role in the field of coal bump prevention and control in coal mines. However, Si et al. [34] proposed a single monitoring and early warning method which only describes the coal bump quantitatively from a specific aspect, due to the variability of coal mines occurrence conditions. The complexity of coal bump, which causes the diversity of coal bump precursor evolution characteristics. For example, the drilling cuttings method can be used to evaluate the coal bump risk and advance stress distribution characteristics of the working face according to the amount of coal powder, drilling depth, and dynamic effect. Nevertheless, this method has the disadvantages of a small monitoring range and poor applicability in the hard coal seam. As a regional monitoring method, acoustic emission (AE) and electromagnetic emission (EME) can be used to realize the monitoring and early warning by monitoring the charging index radiated to the outside space during the coal rock fracture (such as pulse number, amplitude, and frequency). However, this method is greatly affected by the field environment [10, 35–38]. Microseismic monitoring can obtain the occurrence time, duration, and energy field changes of coal bumps. However, He et al. [39] pointed out microseismic monitoring is mostly a postevent record, which is difficult to be used for coal bump prediction. Generally speaking, the early warning of coal bump is a multidimensional problem, and the formation, start-up, and disaster process of coal bump is hardly reflected in a comprehensive way by a single parameter [40, 41]. Comparative analysis of the early warning effectiveness between the new method and the original method used in the working face by the R-score method shows that the R values by the two methods are, respectively, 0.673 and 0.072, which indicates that the new method is far superior to the original method [42]. As a result, it is difficult to improve the accuracy of a single monitoring and early warning index in the field application. At present, the monitoring data of coal bump obtained by different monitoring and warning methods should be analyzed in depth, and the establishment of multiparameter, multilevel, and whole time-space coupling monitoring and early warning is one of the important research directions of coal bump.

Through the microseismic, AE, and EME on-site monitoring, the time-series evolution law of coal bump precursor signals was obtained in this study. The AE and EME parameter concentration index S was constructed by using covariance matrix and principal component analysis. Combined with the microseismic monitoring index, the static and dynamic coal bump risk assessment method was established and applied comprehensively in the subsequent mining of the working face 311305 in a coal mine of Inner Mongolia.

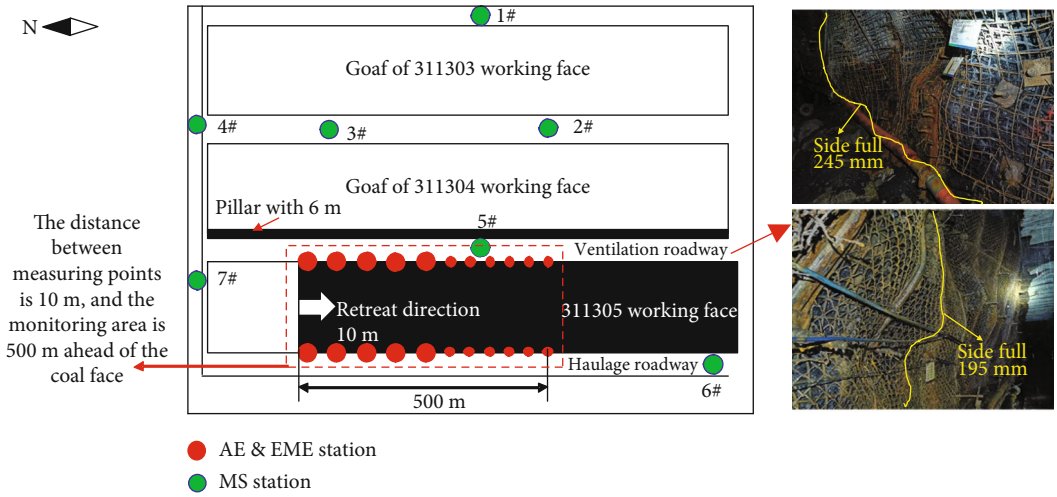

Figure 2: Position of the working face 311305 and layout of measuring points.

2. Geological and Mining Conditions

2.1. Introduction of the Working Face. The Bayangaole coal mine belongs to the Hujierte coalfield. It is located in the Inner Mongolia Autonomous Region, China. The coal-bearing strata were middle Jurassic coal layer. The average buried depth of the working face 311305 was 650 m, with the length of 2460 m and width of 300 m. It was adjacent to 311304 goaf in the east and entity coal in the west (see Figure 2); a coal pillar with a width of 6 m was reserved between the working face and the upper goaf. Extra-thick coal seam (3 No. coal seam) with average thickness of 5.80 m has dip angles ranging from 3° to 6°. The coal hardness coefficient f is 2 ~ 3. Fully mechanized long wall mining method was used to extract the coal seam, and the gob-side entry retaining technology was adopted. The deformation of two sides in the ventilation roadway near the goaf was serious, and the side full was 195-245 mm. Figure 3 shows the comprehensive borehole columnar of the working face. The immediate roof of the coal seam was sandy mudstone with a thickness of 5.89 m, the uniaxial compressive strength of the immediate roof measured in the laboratory was 25.62 MPa, and the main roof was the fine sandstone with a thickness of 18.6 m.

2.2. Microseismic, AE, and EME Monitoring Scheme. The Seismological Observation System (SOS) microseismic monitor device imported from Poland was installed to monitoring seismicity continuously in the Bayangaole coal mine. This system can dynamically monitor the vibration waveform from a long distance in real-time and record the source position, energy level, and duration for subsequent analysis. The geophones are uniaxial with frequency of 1 ~ 600 Hz, sampling rate of 500 Hz, maximum data transmission rate of 1 MB/s, and 16-bit A/D conversion. There are seven microseismic monitoring probes (green spots in Figure 2) in panel, which can well cover the target study area. The type YDD-16 acoustic emission and electromagnetic emission monitoring instrument for coal and rock dynamic disasters was used. The AE and EME measuring points (red points in Figure 2) were arranged in the ventilation roadway and haulage roadway, which was near the production side within 500 m ahead of the coalface; the distance between the two adjacent measuring points was 10 m. To minimize the impact of on-site production on the AE and EME signals, the monitoring time was set in the maintenance shift.

3. Analysis of Monitoring Results

3.1. MS Monitoring Results. Figure 4 shows the time-series curve of vibration energy and frequency monitored by the MS system of the working face 311305 from Aug 1 to Aug 31. The results of MS monitoring show that a strong coal bumps with the energy of more than 1.6×10^5 J occurred in the working face 311305 on August 7. Before the rock occurred, the time-series curve of the MS energy is relatively gentle, and the vibration frequency curve shows an upward trend. It indicates that before the occurrence of coal bump, the elastic energy accumulated in the coal rock is less exchanged with the external space, and the energy released by the microfracture in the coal rock is almost negligible compared with the originally accumulated elastic energy in the coal rock. However, the microfracture events in the coal rock gradually increase, and the microvibration is active. When the energy accumulation of coal rock exceeds the critical value needed for coal bump, the energy is released instantly, and the strong coal bump is caused. In active period, energy quiet existed and sustained 3 ~ 5 days, but the seismic vibration frequency showed a remarkable rising trend, and rock burst/coal bumps always occurred after tremor number decrease.

On Aug 14, 20 and 29, coal bumps with energy over 1.2×10^5 J were detected. Before the occurrence of coal bumps, the microseismic energy curve and frequency curve show a similar fluctuation law as that on Aug 7. Before the microvibration in coal rock changing from active period to declining period, the vibration frequency is more than 15 times. Subsequently, strong coal bumps occur, vibration frequency decreases significantly, and the microseismic energy curve shows an obvious downward trend with the energy

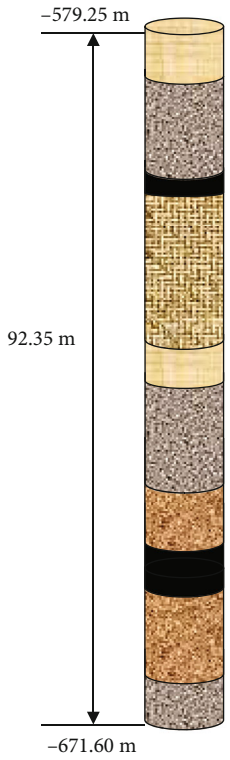

Lithology	Thickness (m)	Remarks
Siltstone	8.80	Dark grey, compact mass, phytolith rich.
Packsand	13.75	Grey to light grey, siliceous cement, rich of siderite stripes and dark grey siltstone stripes.
2# Coal	0.30	Black, semi-bright, stereoplasm, mainly consisting of lump coal.
Medium sandstone	23.00	Grey, mainly consisting of quartz, siliceous cement, harder.
Siltstone	4.61	Dark grey, compact mass, phytolith rich.
Packsand	18.60	Grey to light grey, siliceous cement, rich of siderite stripes and dark grey siltstone stripes.
Sandy mudstone	5.89	Gray, thin laminated, horizontal textured, hard
3# Coal	5.80	Black, semi-bright, stereoplasm, mainly consisting of lump coal.
Sandy mudstone	8.15	Gray, thin laminated, horizontal textured, hard
Packsand	3.45	Grey to light grey, siliceous cement, rich of siderite stripes and dark grey siltstone stripes.

Figure 3: Bore histogram: 311305 coal face.

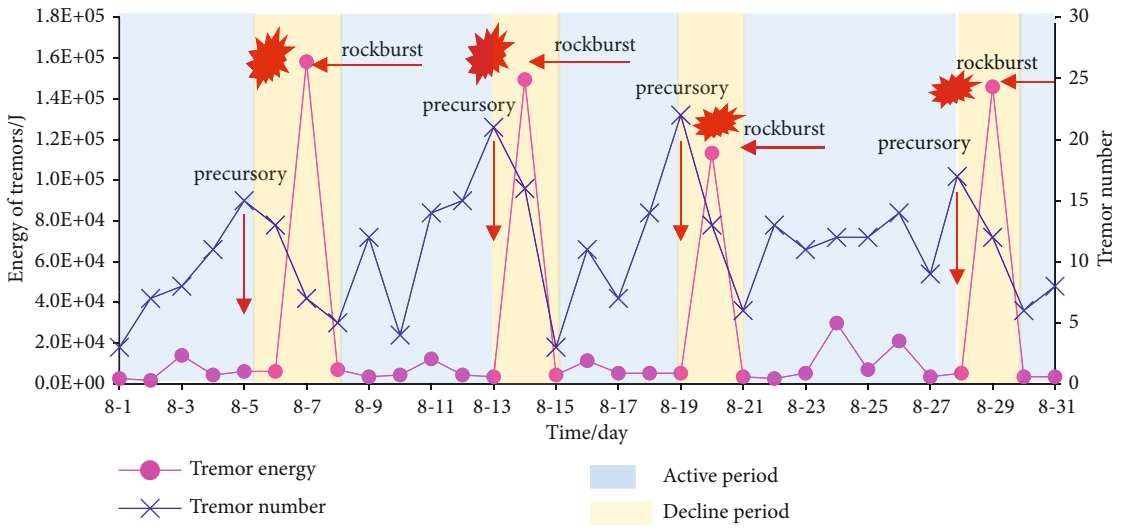

Figure 4: Time-series diagram of MS energy and frequency from Aug 1 to 31.

release. In general, when the vibration frequency curve is maintained at a high value (>15 times) and the total energy curve of the source appears a long stationary period (3 ~ 5d), there is a greater possibility of coal bumps in the working face.

3.2. AE and EME Monitoring Results. As shown in Figure 5, the time-series curve of AE and EME strength at 12 # measuring point, which was arranged ahead of the working face 311305. It can be seen that the AE and EM strength of this measuring point continues to rise within 3-4 days before the coal bump event on Aug 7, 14, 20, and Aug 29. The peak value of AE strength is 1.87-2.39 times of the average value, and the peak value of EME strength is 1.57-2.28 times of the average value. This process is called "active period of AE & EME signals." Subsequently, a strong coal bump occurs in the working face. After the coal bump, the strength of AE

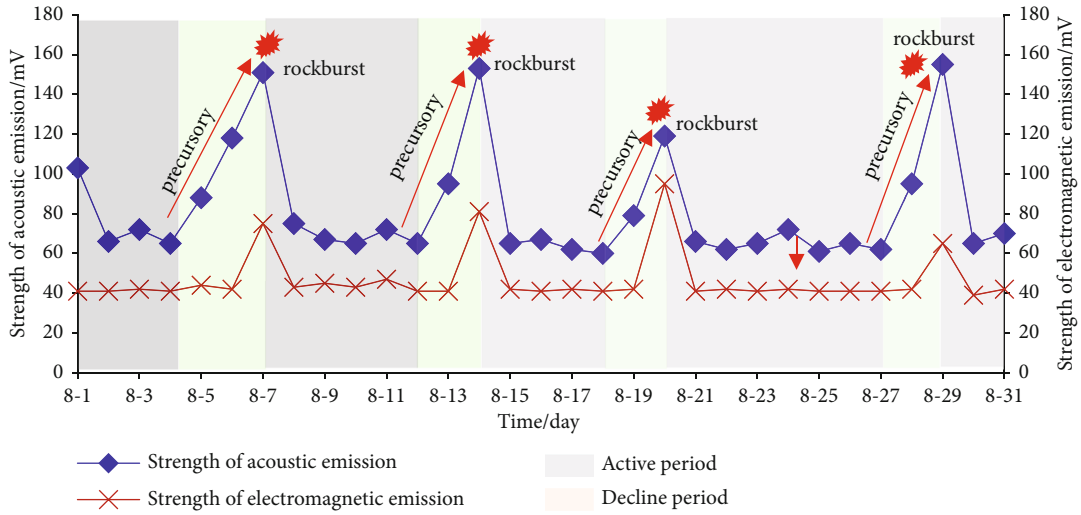

Figure 5: Time-series curve of AE and EME from Aug 1 to 31.

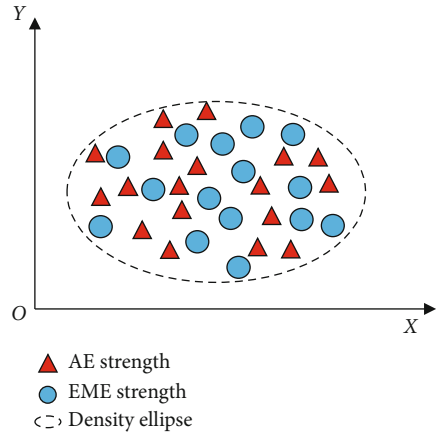

Figure 6: Schematic diagram of density ellipse.

and EME falls back to the normal value, and the time-series curve of AE and EME strength enters the "quiet period of AE & EME signals." Figure 5 also shown the EME strength curve is relatively stable on the whole, and the fluctuation is only observed before the occurrence of coal bump, while the AE strength curve fluctuates up and down with the increase of near-field stress concentration of coal rock and the occurrence of microfracture events. Therefore, the single use of AE strength or EME strength has certain limitations for the early warning of coal bump.

3.3. Multiparameter Coupling Analysis Method. Based on the above analysis, in the monitoring and early warning of coal bump, the energy dissipation and output of coal rock in the advanced area of mining face can be judged by the microseismic monitoring. The internal stress concentration of coal rock in the near field can be judged by the AE and EME signal analysis; then, a qualitative and quantitative evaluation of the risk of coal bump in the advanced area of the working face can be obtained.

Firstly, two measured physical quantities, AE strength and EME strength, are normalized. Assuming that the stress concentration and fracture degree of coal and rock increase in a certain area, the AE signals and EME signals generated in this area will also increase, and then a signal emission group will be formed [43]. The AE strength is represented by vector X, the EME strength is represented by vector Y, and the concentration C is used to describe the distribution of AE signals and EME signals in coal rock. In other words, the fracture area is taken as the center, and the measured X and Y are distributed around the center. The deviation from the center can be described by the covariance matrix, as shown in Eq. (1).

$$C = \begin{pmatrix} c_{11} & c_{12} \\ c_{21} & c_{22} \end{pmatrix}, \tag{1}$$

where

$$\begin{aligned} C_{11} &= E\{[X - E(X)^2]\}, \\ C_{12} &= E\{[X - E(X)][Y - E(Y)]\}, \\ C_{21} &= E\{[X - E(Y)][Y - E(X)]\}, \\ C_{22} &= E\{[Y - E(Y)^2]\}, \end{aligned} \tag{2}$$

and $E(X), E(Y)$ represents the mathematical expectation of vectors X and Y, respectively.

The concentration of acoustic and electrical signals cannot be quantitatively analyzed by the sole use of a covariance matrix. In this study, the principal component analysis method is used to solve the principal component and direction of the distribution of acoustic and electrical signals, and the density ellipse formed by acoustic and electrical signals is used to envelop the acoustic and electrical signals points (see Figure 6). The two principal axes and directions of the density ellipse are determined by the eigenvalues and eigenvectors of the covariance matrix. The larger the area of the density ellipse used for enveloping signals points, the more discrete the concentration of acoustic and electrical signals,

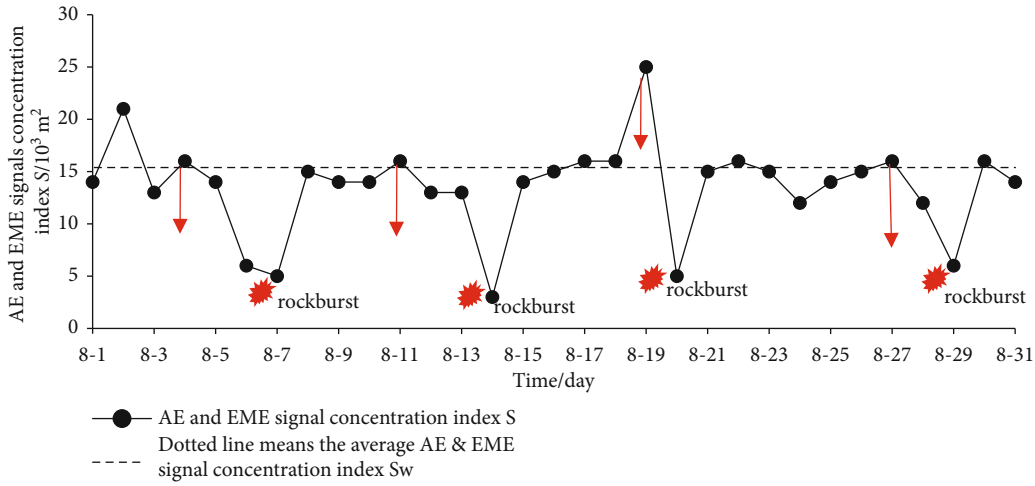

Figure 7: The concentration index S of the AE and EME strength from Aug 1 to 31.

Table 1: Static evaluation method of AE-EME-MS coupling monitoring.

Microseismic index	The concentration index S of acoustic and electrical signals			
	No risk: level A $S > 1.1, S_w$	Weak risk: level B $1.1\ S_w < S < 0.8, S_w$	Medium risk: level C $0.5\ S_w < S < 0.8, S_w$	Strong risk: level D $S < 0.5, S_w$
E: $<10^3$J N: <5	A	A	B	C
E: 10^3-10^4 J N: <5	A	B	B	C
E: $1 - 5 \times 10^4$ J N: 5-10	B	C	D	D
E: $5 - 10 \times 10^4$ J N: 10-15	C	C	D	D
E: $>1.6 \times 10^5$ J N: >15	D	D	D	D

Note: S refers to the concentration index of acoustic and electrical signals during mining, S_w is the average value of concentration index of acoustic and electrical signals, E is the total energy of microseisms, and N is the frequency of microseisms.

and vice versa. And the formula for calculating the area of the density ellipse is shown in Eq. (3).

$$S = \pi\sqrt{C_{11}C_{22} - C_{12}{}^2}, \tag{3}$$

where

$$\begin{aligned} C_{11} &= E\{[X - E(X)^2]\}, \\ C_{12} &= E\{[X - E(X)][Y - E(Y)]\}, \\ C_{22} &= E\{[Y - E(Y)^2]\}, \end{aligned} \tag{4}$$

Equation (3) is used to calculate the concentration index S of AE and EME signal concentration at 311305 working face. The time-series curve of concentration index S during mining in Aug is shown in Figure 7. Before the occurrence of coal bumps, the time-series curve of the concentration index S of AE and EME signals deviates significantly from the average concentration index S_w (S_w dotted line in Figure 7), showing an obvious decreasing trend. When the fracture occurs in the coal rock, the smaller the concentration index S of AE and EME signals, the more concentrated the area of AE and EME signals radiate outward. Accordingly, the higher the stress concentration in this area, the greater the possibility of coal bump. The concentration index S of the AE and EME signals can be used as a comprehensive index for coal bump AE and EME monitoring and early warning.

Table 2: Dynamic evaluation method of AE-EME-MS coupling monitoring.

Duration of continuous enhancement of microseismic activity	Static hazard level			
	A	B	C	D
1d	A	B	C	D
2d	B	C	C	D
3d	B	C	D	D
More than 3d	Danger level is increased by 1 level			

Note: the enhancement of microseismic activity refers to the continuous increase of microseismic frequency.

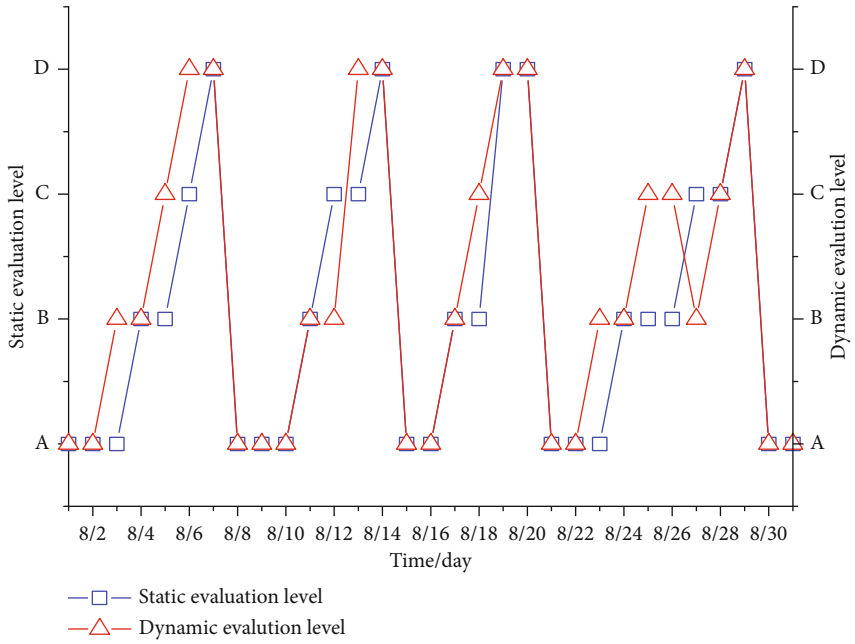

Figure 8: Coal bump risk assessment level from Aug 1 to 31.

Table 1 shows the static evaluation method of coal bump combined with the concentration index S of acoustic and electrical signals and microseismic monitoring index E and N, and Table 2 shows the dynamic evaluation method of AE-EME-MS coupling monitoring. The enhancement of microseismic activity means that the microseismic frequency monitored on the same day is higher than the average value of the microseismic frequency in the first 1-3 days. As shown in Figure 8, the time-series curves of coal bump risk assessment grade of the working face 311305 in Aug are obtained by the static method and dynamic method of the AE-EME-MS coupling monitoring in Tables 1 and 2. It can be seen that the near-field stress distribution, energy accumulation, and release of coal rock are considered simultaneously in the AE-EME-MS coupling monitoring method, and the risk of coal bump in situ can be effectively evaluated by the proposed monitoring method.

4. Discussion

The above research shows that the time-series curves of microseismic energy, microseismic frequency, and the concentration index of acoustic and electrical signals S can be used to characterize the coal bump risk in the working face. According to the time-series curve of AE and EME strength, the time-series curve of concentration index S, the time-series curve of microseismic energy, and the precursor characteristics of strong coal bumps can be determined as follows:

(1) Under the influence of mining stress, the state of the surrounding rock system will evolve to a new stable state over time. Therefore, the surrounding rock near the working face can be regarded as an open system, and the accumulated elastic potential energy, gravity potential energy, and tectonic stress are transmitted to the outside in the form of vibration, acoustic wave, and electromagnetic emission under the influence of mining. Therefore, when the time-series curves of vibration energy, vibration frequency, and AE and EME strength fluctuate violently, the stress concentration and fracture degree in coal rock increase correspondingly, which is the precursor of the strong mine earthquake

(2) When the energy output of the open system composed of surrounding rock near the working face is kept at a low level or has a certain downward trend, the working face has a strong risk of coal bump. Correspondingly, when the time-series curve of microseismic energy at the working face usually presents a stable period of energy fluctuation for 3 - 5 days or has a certain downward trend, and the microseismic frequency time-series curve is in the obvious rising stage and maintains at a high level (>15 times), then the working face has a strong coal bump risk

(3) The concentration index of acoustic and electrical signals deviates obviously from the average curve, showing a downward trend. The time-series curve of AE strength fluctuates obviously, which indicates that the microfracture in coal rock is concentrated in a small area at this time. The smaller the concentration index S, the greater the internal stress concentration in this area, and the higher possibility of a strong coal bumps occurring in the working face

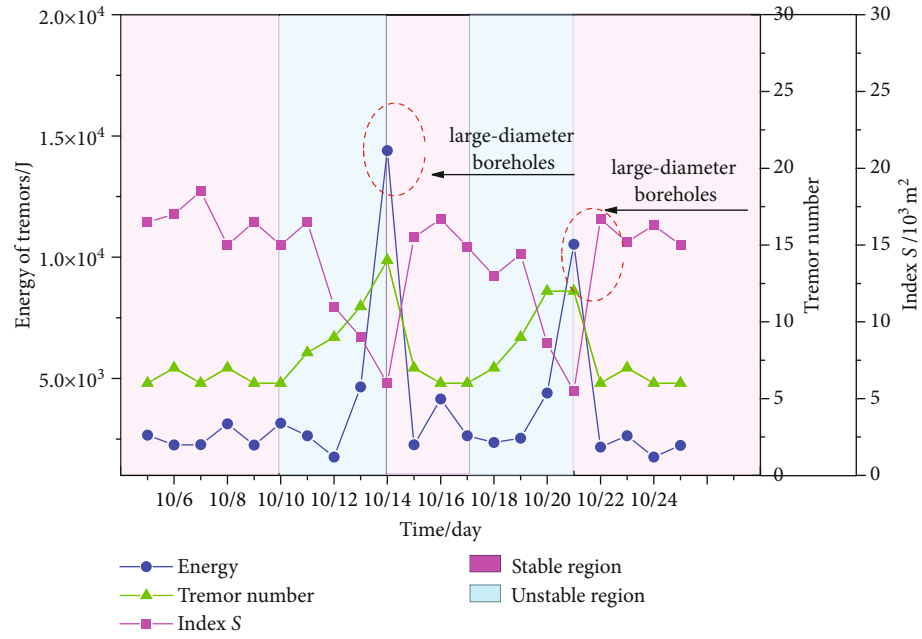

(a) Application of multiparameter coupling early warning method

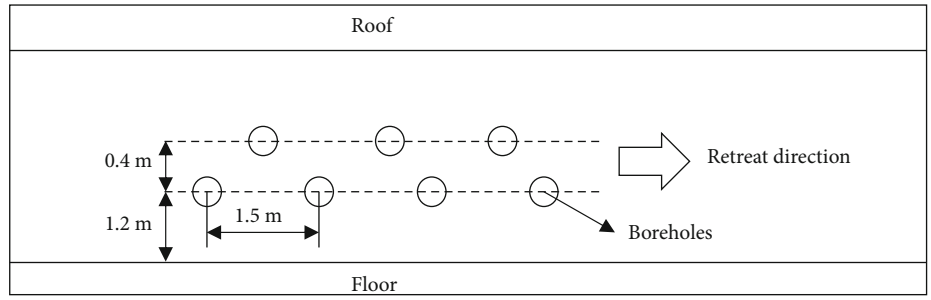

(b) Main view of large-diameter boreholes layout

Figure 9: Application of multiparameter coupling monitoring from Oct 5 to 25.

5. Field Application and Prevention Measures for Coal Bumps

To test the applicability of the AE-EME-MS coupling monitoring method, during the mining period of the working face 311305 in Oct, AE and EME monitoring points were also arranged in the area 400 m ahead of the working face for continuous monitoring. The time-series curves of microseismic energy, vibration frequency, and concentration of acoustic and electrical signals were obtained, as shown in Figure 9(a). From Oct 10 to 13, the monitored time-series curve of microseismic energy on-site first decreased and then increased, the vibration frequency curve showed an obvious increasing trend, and the time-series curve of the concentration index S showed a downward trend. Combined with the monitoring and early warning methods of coal bump given in Tables 1 and 2, it was judged that there was a high probability of coal bump event in the working face 311305 near Oct 14. After that, the large-diameter boreholes were used in the coal seam in the nonproduction side of the transportation roadway 311305 for pressure relief (Figure 9 (b)). The diameter of boreholes was Φ150 mm, the borehole was arranged at a distance of 1.2-1.6 m from the bottom floor, the drilling depth was 15.0 m, and the row spacing was 1.5 m × 0.4 m. After the pressure relief measures were taken, the AE monitoring data was reduced to 65 mv, the EME monitoring data was reduced to 41 mV, and the microseismic energy monitoring data was reduced to 2263 J. According to the same early warning method, another early warning of coal bump was carried out on Oct 21. Through the above field practice, it can be seen that the multiparameter coupling monitoring and early warning method proposed in this study can make a good prediction of coal bump and significantly reduce the probability of coal bump accidents.

6. Conclusion

The occurrence of coal bump is the result of the accumulation and sudden release of elastic properties of coal rock. During the fracture process of coal rock, abundant acoustic and electrical signals can be observed, and the abnormal change of acoustic and electrical signals can be regarded as the precursor characteristics of coal bump.

Before the occurrence of coal bump, there are obvious precursors of acoustic emission and electromagnetic emission-microseism. Specifically, the total energy time-series curve of microseisms is at a low level and relatively stable; the vibration frequency time-series curve has an obvious upward trend; the AE strength time-series curve fluctuates obviously 3-4 days before the occurrence of coal bump, and the AE and EME strength is about 2 times of the normal value.

The area of density ellipse can be used to represent the area of acoustic and electrical signals emitted from coal rock; the covariance matrix and principal component analysis method can be used to construct the concentration index S of acoustic and electrical signals, which can effectively reflect the concentration change of acoustic and electrical signals of coal rock. The smaller concentration index S of acoustic and electrical signals indicates that the microfracture in coal rock is concentrated in a smaller area, and the corresponding stress concentration degree in this area is greater. When the time-series curve of the concentration index S of the acoustic and electrical signals of the working face shows an obvious downward trend and $S < 0.5S_w$, the working face will have a large probability of a strong mine earthquake.

Combined with the variation law of concentration index S of acoustic and electrical signals and microseismic monitoring index value (total energy and frequency of microseisms), the early warning method of AE-EME-MS multiparameter coupling monitoring is proposed. Combined with the pressure relief measures of large diameter borehole implemented in the field, the possibility of coal bump in thick coal seam with the hard roof is greatly reduced, and the effectiveness of the proposed methods with the static evaluation and dynamic early warning of coal bump is verified. This study provides an effective method for the subsequent mining of working face 311305 and early warning and prevention of coal bump on the succeeding working face.

Data Availability

The data of this manuscript is tested in the laboratory of State Key Laboratory of Coal Resources and Safe Mining, China University of Mining and Technology, which is available to authorized users.

Conflicts of Interest

The authors declare that they have no conflicts of interest.

Acknowledgments

We thank Dr. Huining Ni and Dr. Mingwei Chen for their fruitful discussions about this work and Huan Jiang and Xuyang Wang for their help in monitoring date analysis of this work. This work was supported by the National Natural Science Foundation of China (grant number 51774268), Key Research and Development Project of Shanxi Province (grant number 20201101009), and the Postgraduate Research and Innovation Projects of Jiangsu Province (grant number KYCX21_2334).

References

[1] L. Dou and X. He, "Theory and technology of rock burst prevention," University of mining and technology press, Xuzhou: China, 2001.

[2] M. C. He, H. P. Xie, S. P. Peng, and Y. D. Jiang, "Study on rock mechanics in deep mining engineering," *China Journal of Rock Mechanical and Engineering*, vol. 24, no. 16, pp. 2803–2813, 2005.

[3] Q. Qi and L. Dou, *Theory and Technology of Rock Burst*, University of mining and technology press, Xuzhou China, 2008.

[4] X. He, B. Nie, W. Chen et al., "Research progress on electromagnetic radiation in gas-containing coal and rock fracture and its applications," *Safety Science*, vol. 50, no. 4, pp. 728–735, 2012.

[5] Y. Jiang and Y. Zhao, "State of the art: investigation on mechanism, forecast and control of coal bumps in China," *Chinese Journal of Rock Mechanicals and Engineering*, vol. 34, no. 11, pp. 2188–2204, 2015.

[6] Y. Jiang, Y. Zhao, H. Wang, and J. Zhu, "A review of mechanism and prevention technologies of coal bumps in China," *Journal of Rock Mechanics and Geotechnical Engineering*, vol. 9, no. 1, pp. 180–194, 2017.

[7] C. Zhang, I. Canbulat, B. Hebblewhite, and C. R. Ward, "Assessing coal burst phenomena in mining and insights into directions for future research," *International Journal of Coal Geology*, vol. 179, pp. 28–44, 2017.

[8] F. Chen, A. Cao, Z. Liang, and Y. Liu, *A coal burst risk assessment model of seismic events based on multiple seismic source parameters: a case study of the Huating Coal Mine, Gansu Province, China*, Nature Resource Research, 2021.

[9] S. Zhang, G. Fan, D. Zhang et al., "Impacts of longwall mining speeds on permeability of weakly cemented strata and subsurface watertable: a case study," *Geomatics, Natural Hazards and Risk*, vol. 12, no. 1, pp. 3063–3088, 2021.

[10] W. Cai, L. Dou, G. Si, A. Cao, J. He, and S. Liu, "A principal component analysis/fuzzy comprehensive evaluation model for coal burst liability assessment," *International Journal of Rock Mechanics and Mining Sciences*, vol. 81, pp. 62–69, 2016.

[11] W. Cai, L. Dou, G. Si et al., "A new seismic-based strain energy methodology for coal burst forecasting in underground coal mines," *International Journal of Rock Mechanics and Mining Sciences*, vol. 123, article 104086, 2019.

[12] F. Cui, T. H. Zhang, and X. P. Lai, "Research on mining disturbance characteristics and productivity of rock burst mines under different mining intensities," *Journal of China Coal Society*, vol. 3, pp. 1–15, 2021.

[13] N. G. W. Cook, "A note on rockbursts considered as a problem of stability," *Journal of the Southern African Institute of Mining and Metallurgy*, vol. 65, pp. 437–446, 1965.

[14] J. A. Hudson, S. L. Crouch, and C. Fairhurst, "Soft, stiff and servo-controlled testing machines: a review with reference to rock failure," *Engineering Geology*, vol. 6, no. 3, pp. 155–189, 1972.

[15] S. P. Singh, "Burst energy release index," *Rock Mechanics and Rock Engineering*, vol. 21, no. 2, pp. 149–155, 1988.

[16] A. M. Linkov, "Rockbursts and the instability of rock masses," *International Journal of Rock Mechanics and Mining Sciences & Geomechanics Abstracts*, vol. 33, no. 7, pp. 727–732, 1996.

[17] J. Wang and H. D. Park, "Comprehensive prediction of rockburst based on analysis of strain energy in rocks," *Tunnelling and Underground Space Technology*, vol. 16, no. 1, pp. 49–57, 2001.

[18] A. Kidybinski, "Bursting liability indices of coal," *International Journal of Rock Mechanics and Mining Sciences*, vol. 18, no. 4, pp. 295–304, 1981.

[19] C. Zhang, I. Canbulat, F. Tahmasebinia, and B. Hebblewhite, "Assessment of energy release mechanisms contributing to coal burst," *International Journal of Mining Science and Technology.*, vol. 27, no. 1, pp. 43–47, 2017.

[20] L. Dou, C. Lu, Z. Mou, Y. Qin, and J. Yao, "Strength weakening theory for rockburst and its application," *Journal of China Coal Society.*, vol. 30, no. 6, pp. 690–694, 2005.

[21] Q. Qi, X. Li, and S. Zhao, "Theory and practices on stress control of mine pressure bumping," *Coal Science and Technology*, vol. 41, no. 6, pp. 1–5, 2013.

[22] Y. Pan, "Disturbance response instability theory of rockburst in coal mine," *Journal of China Coal Society*, vol. 43, no. 8, pp. 2091–2098, 2018.

[23] Y. S. Pan, Y. H. Xiao, L. I. Zhong-Hua, and K. X. Wang, "Study of tunnel support theory of rockburst in coal mine and its application," *Journal of China Coal Society*, vol. 39, no. 2, pp. 222–228, 2014.

[24] A. Sainoki and H. S. Mitri, "Dynamic behaviour of mining-induced fault slip," *International Journal of Rock Mechanics and Mining Sciences*, vol. 66, pp. 19–29, 2014.

[25] K. Yang, W. J. Liu, L. T. Dou, X. L. Chi, Z. Wei, and Q. Fu, "Experimental investigation into interface effect and progressive instability of coal-rock combined specimen," *Journal of China Coal Society*, vol. 45, no. 5, pp. 1691–1700, 2020.

[26] G. Fan, D. Zhang, and X. Wang, "Mechanism of roof shock in longwall coal mining under surface gully," *Shock and Vibration*, vol. 2015, 8 pages, 2015.

[27] S. T. Gu, C. Q. Wang, B. Y. Jiang, Y. L. Tan, and N. N. Li, "Field test of rock burst danger based on drilling pulverized coal parameters," *Disaster Advances*, vol. 5, no. 4, pp. 237–240, 2012.

[28] X. C. Qu, F. X. Jiang, Z. X. Yu, and H. Ju, "Rockburst monitoring and precaution technology based on equivalent drilling research and its applications," *Chinese Journal of Rock Mechanicals and Engineering*, vol. 30, no. 11, pp. 2346–2351, 2011.

[29] J. He, L. Dou, S. Gong, J. Li, and Z. Ma, "Rock burst assessment and prediction by dynamic and static stress analysis based on micro-seismic monitoring," *International Journal of Rock Mechanics & Mining Sciences*, vol. 93, pp. 46–53, 2017.

[30] V. Frid and K. Vozoff, "Electromagnetic radiation induced by mining rock failure," *International Journal of Coal Geology*, vol. 64, no. 1-2, pp. 57–65, 2005.

[31] E. Wang, X. He, X. Liu, Z. Li, C. Wang, and D. Xiao, "A non-contact mine pressure evaluation method by electromagnetic radiation," *Journal of Applied Geophysics*, vol. 75, no. 2, pp. 338–344, 2011.

[32] N. Hosseini, K. Oraee, K. Shahriar, and K. Goshtasbi, "Studying the stress redistribution around the longwall mining panel using passive seismic velocity tomography and geostatistical estimation," *Arabian Journal of Geosciences*, vol. 6, no. 5, pp. 1407–1416, 2013.

[33] L. M. Dou, W. Cai, S. Y. Gong, R. J. Han, and J. Liu, "Dynamic risk assessment of rock burst based on the technology of seismic computed tomography detection," *Journal of China Coal Society*, vol. 39, no. 2, pp. 238–244, 2014.

[34] G. Si, W. Cai, S. Wang, and X. Li, "Prediction of relatively high-energy seismic events using spatial–temporal parametrisation of mining-induced seismicity,Prediction of relatively high-energy seismic events using spatial–temporal parametrisation of mining-induced seismicity," *Rock Mechanics and Rock Engineering*, vol. 53, pp. 1–22, 2020.

[35] E. Y. Wang, X. F. Liu, X. Q. He, and Z. H. Li, "Acoustic emission and electromagnetic radiation synchronized monitoring technology and early-warning application for coal and rock dynamic disaster," *Journal of China University of Mining and Technology*, vol. 47, no. 5, pp. 942–948, 2018.

[36] Z. L. Li, X. Q. He, L. M. Dou, G. F. Wang, D. Z. Song, and Q. Lou, "Bursting failure behavior of coal and response of acoustic and electromagnetic emissions," *Chinese Journal of Rock Mechanics and Engineering*, vol. 38, no. 10, pp. 2057–2068, 2019.

[37] C. Lu, L. Dou, and X. Wu, "Pt catalyst supported on multi-walled carbon nanotubes for hydrogenation- dearomatization of toluene," *Chinese Journal of Rock Mechanics and Engineering*, vol. 28, no. 3, pp. 210–216, 2007.

[38] L. Dou, W. Cai, A. Cao, and W. Guo, "Comprehensive early warning of rock burst utilizing microseismic multi- parameter indices," *International Journal of Mining Science and Technology*, vol. 28, no. 5, pp. 767–774, 2018.

[39] H. He, L. Dou, S. Gong, J. He, Y. Zheng, and X. Zhang, "Microseismic and electromagnetic coupling method for coal bump risk assessment based on dynamic static energy principles," *Safety Science*, vol. 114, pp. 30–39, 2019.

[40] C. Wang, A. Cao, C. Zhang, and I. Canbulat, "A new method to assess coal burst risks using dynamic and static loading analysis," *Rock Mechanics and Rock Engineering*, vol. 53, no. 3, pp. 1113–1128, 2020.

[41] S. Li, G. Fan, D. Zhang et al., "Fracture propagation and hydraulic properties of a coal floor subjected to thick-seam longwalling above a highly confined aquifer," *Geofluids*, vol. 2021, Article ID 6668466, 12 pages, 2021.

[42] X. Tian, Z. Li, D. Song et al., "Study on microseismic precursors and early warning methods of rockbursts in a working face," *Chinese Journal of Rock Mechanics and Engineering*, vol. 39, no. 12, pp. 2471–2482, 2020.

[43] Y. A. N. G. Chundong, G. O. N. G. Siyuan, M. A. Xiaoping, and W. A. N. G. Guifeng, "Rock burst danger monitoring based on microseismic method," *Journal of Mining & Safety Engineering*, vol. 31, no. 6, pp. 863–868, 2014.